

#2332 THE INSTITUTE OF PAPER CHEMISTRY  
(Rheology of Papermaking Materials)  
Project Reports (2)

PROJECT REPORT

Copies to: Files  
Mr. Swanson  
Dr. Sears  
Dr. Kurath  
Dr. Riemen  
Reading Copy  
10 Extra Copies

Project No. 2332  
Cooperator: Institute  
Report No. 4  
Date February 22, 1965  
Notebook 2172  
Page 40 to 56  
Signed

*S. F. Kurath*  
S. F. Kurath

*W. P. Riemen*

W. P. Riemen

DERIVATION OF THE RABINOWITSCH EQUATION FOR FLOW THROUGH  
CYLINDRICAL TUBES AND ITS APPLICATION TO THE  
NON-NEWTONIAN FLOW OF COATING COLORS

INTRODUCTION

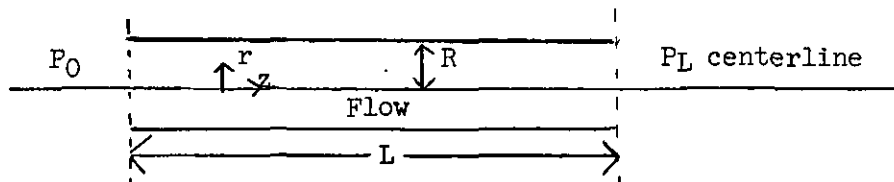
Within the Institute, there has been some objection to the use of capillary viscometry in the study of non-Newtonian flow of fluids. This is most unfortunate since capillary flow is one of the few techniques suitable for studying the flow of fluids at high shear rates. Indeed, properly conducted experiments in capillary viscometers will yield non-Newtonian flow curves in excellent quantitative agreement with measurements taken on concentric cylinder and cone and plate viscometers (1).

In discussing capillary viscometry with a number of our staff members, we found that the main objection has centered about the belief that capillary flow measurements must be restricted to Newtonian fluids if velocity profiles are to be obtained. Some 36 years ago Rabinowitsch (2) indicated how a plot of momentum flux versus velocity gradient could be obtained, for any fluid, simply from a plot of pressure drop versus flow rate obtained from isothermal flow through circular tubes. The Rabinowitsch results have been used by rheologists for many years and have been tested extensively. In view of our institutional interest in non-Newtonian flow, we feel that it would be of interest to present a detailed derivation of the Rabinowitsch equation and some

experimental evidence which tends to confirm its applicability and usefulness in dealing with non-Newtonian liquids at high rates of shear.

### DERIVATION OF THE RABINOWITSCH EQUATION

We consider flow through a cylindrical tube of length,  $L$ , radius,  $R$ , under an applied pressure gradient  $\Delta P = P_0 - P_L$  ( $P_0 > P_L$ ) as shown in the following diagram.



We will attempt to use the notation of Bird et al (3). The velocity has the components  $V_z$ ,  $V_r$  and  $V_\theta$  since we are dealing here in cylindrical coordinates. The momentum fluxes have the components  $\tau_{zz}$ ,  $\tau_{rr}$ ,  $\tau_{\theta\theta}$ ,  $\tau_{rz}$ ,  $\tau_{r\theta}$  and  $\tau_{z\theta}$ . The following assumptions are made:

1. The fluid is incompressible.
2. The flow is taking place isothermally.
3. The flow is taking place under steady state conditions.

This means that  $V_z$ , the velocity in the direction of flow, is constant with respect to time.

4. The flow is laminar, i.e.,  $V_r$  and  $V_\theta$  the components of velocity in the radial and  $\theta$  directions, are zero.
5. There are no entrance or exit effects.
6.  $(V_z)_R$ , the velocity at wall of the tube, is zero.

7.  $-\frac{\partial v_z}{\partial r} = f(\tau_{rz})$ . This assumption means that the viscous momentum flux is in the direction of negative velocity, that the rate of shear is a function of viscous momentum flux only and that it is a function of the liquid itself and does not depend on the radius, R, of the particular tube used in the experiment.
8. The force of gravity is neglected.
9.  $\tau_{zz}$  is not a function of z.

First, we derive an equation for the total volume rate of flow in terms of the rate of shear. The linear velocity,  $v_z$ , at a distance r from the center line is given by,

$$v_z(r) = \int_R^r \frac{\partial v_z}{\partial r} dr = \int_R^r -f(\tau_{rz}) dr \quad (1)$$

Then the total volume rate of flow, Q, is given by

$$Q = \int_0^R v_z(2\pi r dr) = 2\pi \int_0^R \left[ \int_R^r -f(\tau_{rz}) dr \right] r dr \quad (2)$$

Equation (2) can be integrated by parts by letting,

$$g = \int_R^r -f(\tau_{rz}) dr \text{ and } h = r dr \quad (3)$$

in the equation of integration by parts;

$$\int g dh = gh - \int h dg \quad (4)$$

Applying these equations to equation (2), we have,

$$Q = 2\pi \left[ \frac{r^2}{2} \int_R^r -f(\tau_{rz}) dr - \int_0^R -f(\tau_{rz}) \frac{r^2}{2} dr \right] = \pi \int_0^R r^2 f(\tau_{rz}) dr \quad (5)$$

Next we must obtain a relation between  $r$  and  $\tau_{rz}$ . We proceed as follows. The equation of motion of a fluid under general conditions is given for the  $z$  component in cylindrical coordinates as follows,

$$\rho \left( \frac{\partial v_z}{\partial t} + v_r \frac{\partial v_z}{\partial r} + \frac{v_\theta}{r} \frac{\partial v_z}{\partial \theta} + v_z \frac{\partial v_z}{\partial z} \right) = - \frac{\partial P}{\partial z} - \left( \frac{1}{r} \frac{\partial}{\partial r} (r \tau_{rz}) + \frac{1}{r} \frac{\partial \tau_{\theta z}}{\partial \theta} + \frac{\partial \tau_{zz}}{\partial z} \right) + \rho g_z \quad (6)$$

In view of the assumptions made previously we can eliminate most of the terms in equation (6). The first term on the left is zero because of the steady state assumption, the second and third are zero because of laminar flow and the fourth is zero because  $\frac{\partial v_z}{\partial z} = 0$  is the equation of continuity of an incompressible fluid when  $v_r$  and  $v_\theta$  are zero. On the righthand side we neglect gravity. The term  $\frac{\partial \tau_{\theta z}}{\partial \theta}$  is zero since there is no dependence of  $\tau_{\theta z}$  on  $\theta$  because of axial symmetry. The term  $\frac{\partial \tau_{zz}}{\partial z}$  is zero because it was assumed that  $\tau_{zz}$  did not depend on  $z$ . Hence, equation (6) reduces to,

$$0 = - \frac{\partial P}{\partial z} - \frac{1}{r} \frac{\partial}{\partial r} (r \tau_{rz}) \quad (7)$$

We next integrate equation (7) with respect to  $z$ ,

$$\int_{P_0}^{P_L} dP = - \frac{1}{r} \frac{\partial}{\partial r} (r \tau_{rz}) \int_0^L dz \quad (8)$$

or,

$$\frac{1}{r} \frac{\partial}{\partial r} (r \tau_{rz}) = \frac{P_0 - P_L}{L} = \frac{\Delta P}{L} \quad (9)$$

Integrating equation (9) with respect to  $r$ , we have,

$$r \tau_{rz} = \frac{r^2 \Delta P}{2L} + \text{constant} \quad (10)$$

The constant in equation (10) is zero since  $r_{rz}^{\tau} = 0$  at  $r = 0$ . Finally, we can rewrite equation (10), as,

$$\tau_{rz} = \frac{r\Delta P}{2L} \quad (11)$$

and

$$(\tau_{rz})_R = \frac{R\Delta P}{2L} \quad (12)$$

and, combining equations (11) and (12),

$$r = R \frac{\tau_{rz}}{(\tau_{rz})_R} \quad (13)$$

We can now substitute equation (13) in equation (5) to obtain,

$$Q = \pi \int_0^{(\tau_{rz})_R} \left( \frac{R}{(\tau_{rz})_R} \right)^3 \tau_{rz}^2 f(\tau_{rz}) d\tau_{rz} \quad (14)$$

We can rearrange equation (14) to give,

$$\frac{Q}{\pi R^3} = \frac{1}{(\tau_{rz})_R^3} \int_0^{(\tau_{rz})_R} \tau_{rz}^2 f(\tau_{rz}) d\tau_{rz} = F[(\tau_{rz})_R] \quad (15)$$

Since we must differentiate equation (15) with respect to  $(\tau_{rz})_R$ , we give the Leibnitz formula (4) for differentiation needed in this case,

$$\frac{d\varphi(\alpha)}{d\alpha} = g(u_1, \alpha) \frac{du_1(\alpha)}{d\alpha} - g(u_0, \alpha) \frac{du_0(\alpha)}{d\alpha} + \int_{u_0(\alpha)}^{u_1(\alpha)} \frac{\partial g(x, \alpha)}{\partial \alpha} dx \quad (16)$$

$$\text{where } \varphi(\alpha) = \int_{u_0(\alpha)}^{u_1(\alpha)} g(x, \alpha) dx \quad (17)$$

If we identify  $\alpha$  with  $(\tau_{rz})_R$ ,  $u_1(\alpha)$  with  $(\tau_{rz})_R$ ,  $u_0(\alpha)$  with 0,  $g(x, \alpha)$  with  $\tau_{rz}^2 f(\tau_{rz})$  and  $\tau_{rz}$  with  $x$  we can differentiate equation (15) with the aid of equations (16) and (17) to obtain

$$\frac{dF[(\tau_{rz})_R]}{d(\tau_{rz})_R} = -\frac{3}{(\tau_{rz})_R} \int_0^{(\tau_{rz})_R} (\tau_{rz})^2 f(\tau_{rz}) d\tau_{rz} + \frac{1}{(\tau_{rz})_R} \left\{ (\tau_{rz})_R^2 f[(\tau_{rz})_R] - 0 + \int_0^{(\tau_{rz})_R} \frac{\partial \{ \tau_{rz}^2 f(\tau_{rz}) \}}{\partial (\tau_{rz})_R} d\tau_{rz} \right\} \quad (18)$$

Since the last term is zero because the partial derivative is zero, equation (18) becomes with the help of equation (15),

$$\frac{d F[(\tau_{rz})_R]}{d(\tau_{rz})_R} = -\frac{3}{(\tau_{rz})_R} F[(\tau_{rz})_R] + \frac{1}{(\tau_{rz})_R} f[(\tau_{rz})_R] \quad (19)$$

Upon rearrangement, we obtain for  $f[(\tau_{rz})_R]$ ,

$$f[(\tau_{rz})_R] = 3F[(\tau_{rz})_R] + (\tau_{rz})_R \frac{dF[(\tau_{rz})_R]}{d(\tau_{rz})_R} \quad (20)$$

$$= 3F[(\tau_{rz})_R] + F[(\tau_{rz})_R] \left[ \frac{d \log F[(\tau_{rz})_R]}{d \log (\tau_{rz})_R} \right] \quad (21)$$

Thus, 
$$f[(\tau_{rz})_R] = F[(\tau_{rz})_R] \left[ 3 + \frac{d \log F[(\tau_{rz})_R]}{d \log (\tau_{rz})_R} \right] \quad (22)$$

At this point we simplify our notation and let,

$$(\tau_{rz})_R = \tau_R$$

and

$$\frac{d \log (\tau_{rz})_R}{d \log F[(\tau_{rz})_R]} = N(\tau_R) = N \quad (23)$$

where  $N$  is the slope of a plot of  $\log \tau_R$  versus  $\log F(\tau_R)$  and is a function of  $\tau_R$  in the general case. Using this notation and equation (15) we rewrite equation (23) as,

$$f(\tau_R) = \frac{Q}{\pi R^3} \left( 3 + \frac{1}{N} \right) = \frac{Q}{\pi R^3} \left( \frac{3N + 1}{N} \right) \quad (24)$$

Now, since the rate of shear for a Newtonian fluid is given by  $\frac{4Q}{\pi R^3}$  it is convenient to rewrite equation (24) as follows,

$$f(\tau_R) = \frac{4Q}{\pi R^3} \left( \frac{3N + 1}{4N} \right) \quad (25)$$

The value of  $N(\tau_R)$  can be obtained from the slope of a plot of  $\log \tau_R$  versus  $\log \frac{4Q}{\pi R^3}$  or from the slope of a plot of  $\log \Delta P$  versus  $\log Q$  since,

$$\frac{d \log \tau_R}{d \log \frac{4Q}{\pi R^3}} = \frac{d \log \tau_R}{d \log \frac{Q}{\pi R^3}} = \frac{d \log \frac{\frac{R\Delta P}{2L}}{\frac{4Q}{\pi R^3}}}{d \log Q} = N \quad (26)$$

Thus, from a knowledge of  $R$  and  $L$  and a plot of  $\Delta P$  versus  $Q$  one can obtain the necessary data for a rheological plot of  $\log \tau_R$  versus  $\log$  rate of shear,  $\log f(\tau_R)$  by utilizing equations (12) and (25).

Equation (25) also enables us to calculate the velocity distribution in the tube as a function of  $r$ . Equation (1) can be written in the following form by the use of equation (13).

$$V_z(r) = \int_{\left(\frac{r}{R}\right)\tau_R}^{\tau_R} \left(\frac{R}{\tau_{rz}}\right) f(\tau_{rz}) d\tau_{rz} \quad (27)$$

$$V_z(0) = \int_0^{\tau_R} \left(\frac{R}{\tau_{rz}}\right) f(\tau_{rz}) d\tau_{rz} \quad (28)$$

Hence,

$$\frac{V_z(r)}{V_z(0)} = 1 - \frac{\int_0^{\left(\frac{r}{R}\right)\tau_R} f(\tau_{rz}) d\tau_{rz}}{\int_0^{\tau_R} f(\tau_{rz}) d\tau_{rz}} \quad (29)$$

But by assumption 7,  $f(\tau_{rz})$  is an intrinsic property of the liquid and is independent of the radius,  $R$ , of the tube used to obtain it. Hence,

$$f(\tau_{rz}) = f(\tau_R) \quad (30)$$

Then, equation (29) becomes

$$\frac{V_z(r)}{V_z(0)} = 1 - \frac{\int_0^{(\frac{r}{R})\tau_R} f(\tau_R) d\tau_R}{\int_0^{\tau_R} f(\tau_R) d\tau_R} \quad (31)$$

The righthand side of equation (31) is a function of  $(r/R)$  and the ratio of integrals can be interpreted as in the following equation,

$$\frac{V_z(r)}{V_z(0)} = 1 - \frac{\text{area under } f(\tau_R) \text{ versus } \tau_R \text{ from } 0 \text{ to } (\frac{r}{R})\tau_R}{\text{area under } f(\tau_R) \text{ versus } \tau_R \text{ from } 0 \text{ to } \tau_R} = g(\frac{r}{R}) \quad (32)$$

Up to this point we have made no assumptions on the nature of  $N(\tau_R)$ . If we are dealing with a power law fluid where  $N(\tau_R)$  is a constant we can use equation (31) to derive an analytic expression for the velocity distribution. We have in this case,

$$\frac{d \log \tau_R}{d \log \frac{4Q}{\pi R^3}} = N' = \text{a constant} \quad (33)$$

Integration of equation (33) yields,

$$\log \tau_R = N' \log \frac{4Q}{\pi R^3} + C \quad (34)$$

or,

$$\tau_R = \left( \frac{4Q}{\pi R^3} \right)^{N'} 10^C = K \left( \frac{4Q}{\pi R^3} \right)^{N'} \quad (35)$$

Then by substituting equation (35) in equation (25),

$$f(\tau_R) = \left( \frac{\tau_R}{K} \right)^{\frac{1}{N'}} \left( \frac{3N'+1}{4N'} \right) \quad (36)$$

Using equation (36) in equation (31), we have,

$$\frac{V_z(r)}{V_z(0)} = 1 - \frac{\int_0^{(r/R)\tau_R} \left(\frac{\tau_R}{K}\right)^{\frac{1}{N'}} \left(\frac{3N'+1}{4N'}\right) d\tau_R}{\int_0^{\tau_R} \left(\frac{\tau_R}{K}\right)^{\frac{1}{N'}} \left(\frac{3N'+1}{4N'}\right) d\tau_R} \quad (37)$$

Performing the integrations indicated above, we have,

$$\frac{V_z(r)}{V_z(0)} = 1 - \left(\frac{r}{R}\right)^{\frac{1}{N'}+1} \quad (38)$$

as the velocity distribution for a power law fluid in terms of  $(r/R)$

In the case of a Newtonian fluid,  $N' = 1$ , and we have,

$$\frac{V_z(r)}{V_z(0)} = 1 - (r/R)^2 \quad (39)$$

which is the parabolic velocity distribution for Newtonian fluids.

#### BEHAVIOR OF CLAY-STARCH COATING COLORS AT HIGH SHEAR RATES

A series of experiments was performed with three clay-starch coating colors using high and low shear capillary viscometers to be described below over an unusually wide range in shear rates from 1.5 to  $1.92 \times 10^5 \text{ sec.}^{-1}$ .

These colors were strongly non-Newtonian and appeared to be good test systems for both the viscometers and the Rabinowitsch equation.

#### Viscometry

The high shear viscometer consisted of a 1 cc. tuberculin syringe with a Yale Luer-lok. The capillary was a no. 24 needle with a blunt tip (the kind used to fill ultracentrifuge cells.) The dimensions of the capillary were: length, 2.5 cm.; inside diameter, 0.0281 cm.; and, length to diameter ratio, 89.

The low shear viscometer was essentially the same as the high shear viscometer except that a 5 cc. syringe was used in conjunction with a no. 16 needle. The dimensions of this capillary were: length, 2.60 cm.; inside diameter, 0.1185 cm.; length to diameter ratio, 22.

The viscometers were mounted on a flexaframe stand and water at 25°C. was circulated around the capillary. Driving pressures for the high shear viscometer were provided by loading the plunger of the syringe by means of a piston arrangement which used beater weights as dead loads. Driving pressures for the low shear viscometer were supplied by air pressure in a mercury manostat and by gravity at the lowest shear rates. The experiments were conducted in these viscometers by measuring the time required to expel 1 cc. of coating color from the syringe under a given load.

Mineral oil (heavy USP 340/350) of known viscosity was used in the calibration of both viscometers. The results of measurements with this oil showed that the viscosity was independent of shear rate up to shear rates of  $7 \times 10^4 \text{ sec.}^{-1}$  indicating that heating effects are not important in these particular viscometers.

#### Coating Color Formulations

The coating colors, prepared by J. D. Hultman, consisted of starch (Superfilm 40), clay (Sp. Hydratex), calcium carbonate (Purecal 0) and Latex (Dow 512R). The three colors used in this study and their exact compositions and designations can be found in Table I. The details of the procedures used to mix the various ingredients can be found in Notebook 2172, pages 44-46.

TABLE I

| <u>Color Number</u>             | <u>1</u> | <u>2</u> | <u>3</u> |
|---------------------------------|----------|----------|----------|
| Special Hydratex (kaolin clay)  | 150 g.   | 270 g.   | 270 g.   |
| Superfilm 40 (starch)           | 27 g.    | 30 g.    | 30 g.    |
| Purecal O (calcium carbonate)   | ---      | 30 g.    | 30 g.    |
| Dow 512R (Latex)                | ---      | 15 g.    | 15 g.    |
| Napco DC-104 (Calcium Stearate) | ---      | ---      | 3.5 g.   |
| Distilled water                 | 177 g.   | 230 g.   | 285 g.   |
| Total Solids, %                 | 50%      | 60%      | 55%      |

RESULTS AND DISCUSSION

One is interested in obtaining a diagram of shear stress at the capillary wall versus velocity gradient (rate of shear) at the wall. We will restate equations (12) and (25) which were used to determine the needed quantities from data involving Q,  $\Delta P$ , R and L.

$$\tau_R = \frac{R\Delta P}{2L} \quad (12)$$

and

$$f(\tau_R) = \frac{4Q}{\pi R^3} \left( \frac{3N + 1}{4N} \right) \quad (25)$$

where  $N(\tau_R)$  is the slope of a double logarithmic plot of  $\tau_R$  versus  $\frac{4Q}{\pi R^3}$ . The necessary data for plots of  $\log \tau_R$  versus  $\log f(\tau_R)$  for the three coating colors found in Figure 1 are exhibited in Table II.

It will be seen from Figure 1 that there was overlapping of data points taken on the high and low shear viscometers in the case of coating 3. This constitutes evidence that assumption 7 was applicable and that  $f(\tau_R)$  is a function of the liquid only and does not depend on the dimensions of the viscometer.

TABLE II  
 SHEAR STRESS AND RATE-OF-SHEAR DATA FOR  
 CLAY-STARCH COATING COLORS

| Coating   | 1  | 2   | 3  |
|---|--|---|--|
| $\tau_R \times 10^{-4}$<br>dynes/cm. <sup>2</sup> | $f(\tau_R) \times 10^{-4}$<br>sec. <sup>-1</sup> | $\tau_R \times 10^{-4}$<br>dynes/cm. <sup>2</sup> | $f(\tau_R) \times 10^{-4}$<br>sec. <sup>-1</sup> |
| * 0.0169  | * 0.00015  | 1.71  | * 0.0772 * 0.0204                                |
| * 0.0386  | * 0.0023   | 2.19  | * 0.186 * 0.0650                                 |
| * 0.0476  | * 0.0076   | 4.52  | * 0.328 * 0.1313                                 |
| * 0.101   | * 0.0272   | 5.88  | * 0.547 * 0.381                                  |
| * 0.161   | * 0.0593   | 8.14  | * 0.725 * 0.596                                  |
| 0.815   | 0.393  | 9.68  | 0.541 0.374                                      |
| 1.72  | 1.23   | 11.9  | 0.541 0.408                                      |
| 2.19  | 1.60   |   | 0.873 0.710                                      |
| 3.53  | 3.41   |   | 1.71 1.92  |
| 4.00  | 4.01   |   | 2.19 2.71  |
| 6.68  | 7.34   |   | 2.79 3.73  |
| 9.55  | 11.4   |   | 4.23 6.41  |
| 13.5  | 19.2   |   |  |

\* Taken on low shear viscometer; unmarked items taken on high shear viscometer.

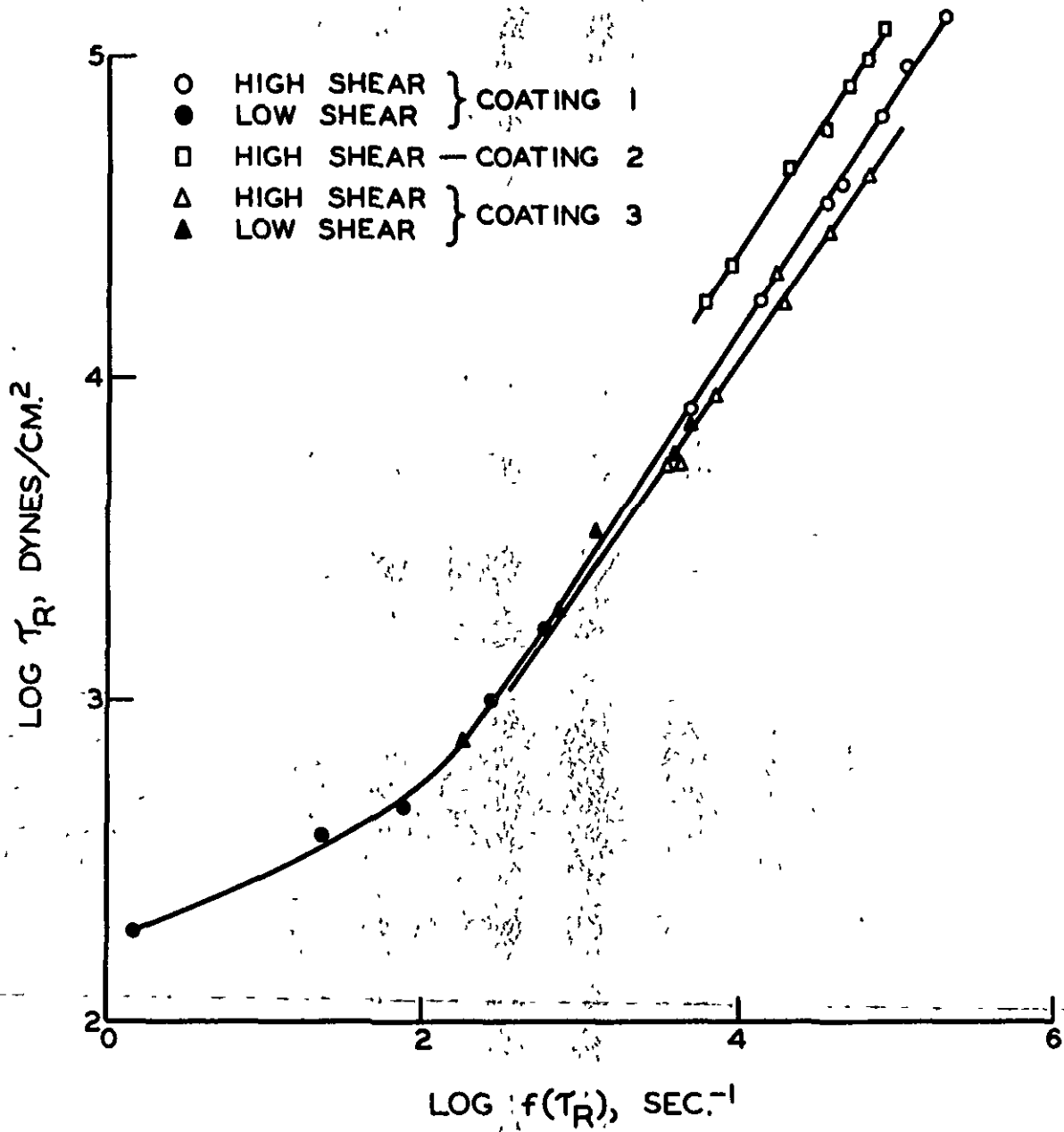


Figure 1. Shear stress versus rate-of-shear for clay-starch coating colors.

It will also be seen from Figure 1 that a straight line relation between  $\log \tau_R$  and  $\log f(\tau_R)$  is obtained at high shear rates for all three coating colors. This means that the high shear rate data can be correlated by a power law equation similar to equation (35),

$$\tau_R = C[f(\tau_R)]^n \quad (40)$$

For coating color 1,

$$\tau_R = 17.5 [f(\tau_R)]^{0.73} \quad (41)$$

where  $\tau_R$  has the units of dynes/cm.<sup>2</sup> and  $f(\tau_R)$  the units of sec.<sup>-1</sup>. The equation is valid over a range of  $f(\tau_R)$  from  $1.2 \times 10^3$  to  $1.9 \times 10^5$  sec.<sup>-1</sup>.

Similar equations can be written for the high shear regions of the other two coating colors. On the basis of past experience (5), it is expected that many non-Newtonian materials can be described by equation (40). This is the familiar Ostwald equation for pseudoplastic fluids.

A velocity profile for coating color 1 was calculated for a shear stress of  $5 \times 10^4$  dynes/cm.<sup>2</sup> at which the rate-of-shear at the wall was  $8.4 \times 10^4$  sec.<sup>-1</sup>. Equation (32) and a plot of  $f(\tau_R)$  versus  $\tau_R$  were used for this purpose. The results are presented in Figure 2. For comparison purposes the parabolic profile for a Newtonian liquid is also shown in Figure 2.

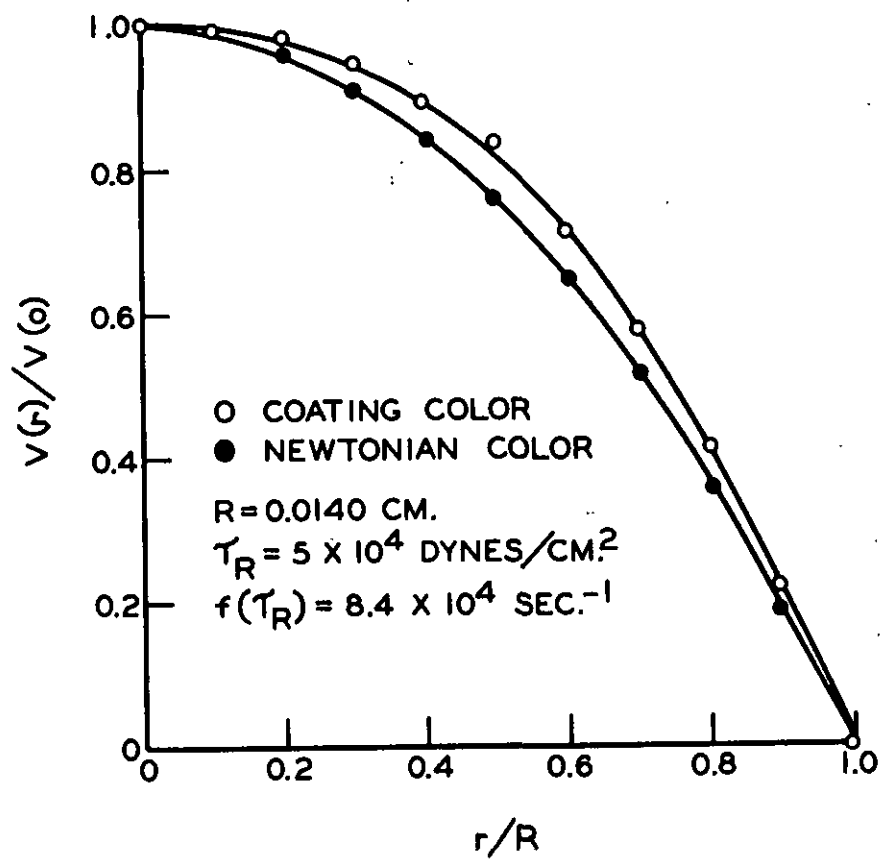


Figure 2. Velocity profile for clay-starch coating color 1.

REFERENCES

1. Brodnyan, J. G., Gaskins, F. H. and Philippoff, W., Trans. Soc. Rheology 2:285 (1958).
2. Rabinowitsch, B., Z. Physik. Chemie A145:1 (1929).
3. Bird, R. B., Stewart, W. E., and Lightfoot, E. N. "Transport Phenomena", New York, John Wiley and Sons, Inc., Chapter 3.
4. Sokolnikoff, I. S. and Sokolnikoff, E. S. "Higher Mathematics for Engineers and Physicists," McGraw-Hill Book Co., New York.
5. Metzner, A. B. and Reed, J. C. Ind. Eng. Chem. 1:434 (1955).

PROJECT REPORT FORM

Project No. 2332 Report 3

Project No. 1695 Report 4

Co-operator I.P.C.

Date March 20, 1964

Signed S. F. Kurath

S. F. Kurath

C. A. Schmitt

C. A. Schmitt

J. J. Bachhuber

J. J. Bachhuber

Copies to: Files  
Swanson  
Ward  
Leekley  
Kurath  
Schmitt  
Bachhuber  
Reading Copy  
Swenson

THE HYDRODYNAMIC BEHAVIOR OF FULLY ACETYLATED GUARAN. A TEST  
OF THE EIZNER-PTITSYN THEORY FOR THE SEMIRIGID MACROMOLECULE

BACKGROUND

The material contained in this report is the result of several phases of institutional research. The experimental data on the hydrodynamic behavior of fully acetylated guaran in acetonitrile is the result of the doctoral thesis work of J. V. Koleske (1). Analysis of this work in terms of the Eizner-Ptitsyn theory (2) is the result of a survey conducted on Project 2332, "The rheology of papermaking materials". Machine computation of the geometric and hydrodynamic functions arising in the Eizner-Ptitsyn theory was the result of a mutual interest in the theory in connection with Project 1695, "Fractionation of cellulose and its degradation products" and Project 2332.

INTRODUCTION

The configuration and hydrodynamic properties of fully acetylated guaran (1), GTA, in acetonitrile have been examined over a range in degree of polymerization from 171 to 12,400. The GTA molecule exhibits a transition from partial to nondraining hydrodynamic behavior and excluded volume effects

have been shown to be negligible. Reliable estimates of the polymolecularity of GTA fractions are available so that suitable tests of current hydrodynamic theories are possible.

Recently Eizner and Ptitsyn (2) have treated the intrinsic viscosity of semirigid macromolecules in light of the intrinsic viscosity equation of Peterlin (3,4) and the "wormlike" chain of Kratky and Porod (5). The hydrodynamic behavior of GTA is such that the conditions under which the theory may be applied are fully satisfied. It is the purpose of the present work to test the Eizner-Ptitsyn theory and to comment on the applicability of the theories of Kirkwood and Riseman (6), Kurata and Yamakawa (7) and of Hearst (8).

#### THE EIZNER-PTITSYN THEORY

The Eizner-Ptitsyn theory (2) is based on the "wormlike" chain model of Kratky and Porod. In this model the chain direction varies continuously instead of at specified bonds and the flexibility of the chain is characterized by the persistence length  $a$ . The mean-square radius-of-gyration,  $\overline{S^2}$ , of the "wormlike" chain is given by,

$$\overline{S^2} = (a^2/3)(x - 1 + e^{-x}), \quad (1)$$

where  $x = Nb/a$  and  $N$  is the degree of polymerization and  $b$  is the length of a monomer unit.

According to the theory of Eizner and Ptitsyn the intrinsic viscosity of the semirigid molecule is given by,

$$[\eta] = \frac{2^{3/2} \Phi_0 (b^3/M_0) N \chi(N/\lambda)}{\frac{45(2\pi/3)^{1/2}}{32(3 - 2^{1/2})} \frac{b}{\lambda r_0} + \frac{1}{\lambda^{3/2}} \varphi(\lambda, N) N^{1/2}} \quad (2)$$

where  $[\eta]$  is the intrinsic viscosity in cc.<sup>3</sup>/g., the limiting value of the Flory coefficient,  $\Phi_0$ , is  $2.86 \times 10^{23}$  mole<sup>-1</sup> at high molecular weight (2),  $r_0$  is the hydrodynamic radius of the monomer unit and  $M_0$  its molecular weight and  $\lambda = a/b$ . The hydrodynamic radius is related to the monomeric friction coefficient  $\zeta$  by,  $r_0 = \zeta / 6\pi\eta_0$  where  $\eta_0$  is the solvent viscosity. The function  $\chi(N/\lambda)$  is a geometric factor and  $\varphi(N, \lambda)$  is a complicated hydrodynamic function.

The Flory coefficient is defined by (9),

$$\Phi = [\eta] M / (6 S^2)^{3/2}, \quad (3)$$

and from the present theory is given by,

$$\Phi = \frac{\Phi_0}{\left[ \varphi(\lambda, N) + \frac{45(2\pi/3)^{1/2}}{32(3 - 2^{1/2})} \frac{b}{r_0} \left(\frac{\lambda}{N}\right)^{1/2} \right]} \chi(N/\lambda) \quad (4)$$

#### CALCULATION OF $\chi(N/\lambda)$ AND $\varphi(\lambda, N)$

The geometric and hydrodynamic functions have been calculated by Eizner and Ptitsyn and are presented in graphical form by these authors (2). Unfortunately, the numerical results of their calculations are not given in tabular form so that their graphical results cannot be easily reproduced. For this reason we have repeated their calculation of these functions and have tabulated the numerical results.

The geometric function  $\chi(N/\lambda)$  is given by,

$$\chi(Z) = 1 - (3/Z^3)[Z^2 - 2(Z - 1 + e^{-Z})], \quad (5)$$

where  $Z = N/\lambda$  and the numerical results based on this equation are given in Table I.

The hydrodynamic function is given by,

$$\begin{aligned} \varphi(\lambda, N) = & \frac{15(\pi/3)^{1/2}}{4(3 - 2^{1/2})} \frac{1}{\lambda^{1/2} N^{5/2}} \left\{ \sum_{k=1}^{N-1} \frac{(k^2 + k - Nk - 2N) \Psi(x)}{[x - 1 + \exp(-x)]^{1/2}} \right. \\ & \left. + \sum_{k=1}^{(N/2) - 1} \frac{[(N^2/2) - 2k^2 + N] \Psi(x)}{[x - 1 + \exp(-x)]^{1/2}} \right\} \quad (6) \end{aligned}$$

where

$$\Psi(x) = 0.4270 + 0.5730 \frac{45x^2 + 156x + 214 - 54(4+x)e^{-x} + 2e^{-3x}}{27[x - 1 + e^{-x}]^2} \quad (7)$$

and  $x = k/\lambda$ . Values of the hydrodynamic function were calculated from Equations (6) and (7) by numerical summation on an IBM 1620 computer with Fortran II programming to avoid truncation errors. The results are given in Table II.

## EXPERIMENTAL RESULTS

### INTRINSIC VISCOSITY AND LIGHT SCATTERING

The intrinsic viscosity and light scattering results given in Table III have been reported previously (1). The intrinsic viscosities are the result of measurements conducted in a capillary viscometer of the Ubbelohde type and where necessary corrections for non-Newtonian flow have been applied. Values for the weight average degree of polymerization were

TABLE I

<sup>a</sup> VALUES FOR THE FUNCTION  $\chi(z)$  FROM THE EIZNER-PTITSYN  
 THEORY FOR THE INTRINSIC VISCOSITY OF SEMIRIGID  
 MACROMOLECULES

| <u>z</u> | $\chi(\underline{z})$ | <u>z</u> | $\chi(\underline{z})$ | <u>z</u> | $\chi(\underline{z})$ |
|----------|-----------------------|----------|-----------------------|----------|-----------------------|
| 1.00     | 0.207                 | 10.0     | 0.754                 | 100      | 0.971                 |
| 1.26     | 0.248                 | 12.6     | 0.800                 | 126      | 0.976                 |
| 1.60     | 0.300                 | 16.0     | 0.835                 | 160      | 0.982                 |
| 2.00     | 0.352                 | 20.0     | 0.864                 | 200      | 0.985                 |
| 2.50     | 0.407                 | 25.0     | 0.889                 | 250      | 0.988                 |
| 3.00     | 0.456                 | 30.0     | 0.906                 | 300      | 0.999                 |
| 4.00     | 0.533                 | 40.0     | 0.929                 |          |                       |
| 5.00     | 0.592                 | 50.0     | 0.942                 |          |                       |
| 6.30     | 0.651                 | 63.0     | 0.954                 |          |                       |
| 8.00     | 0.707                 | 80.0     | 0.963                 |          |                       |

<sup>a</sup> Values calculated from Equation (5).

TABLE II

THE FUNCTION  $\varphi(\lambda, N)$  FROM THE EIZNER-PTITSYN THEORY  
 FOR THE INTRINSIC VISCOSITY OF SEMIRIGID MOLECUCULES<sup>a</sup>

| $N$    | $\lambda = 1$ | $\lambda = 5$ | $\lambda = 10$ | $\lambda = 15$ | $\lambda = 20$ | $\lambda = 30$ | $\lambda = 50$ | $\lambda = 100$ |
|--------|---------------|---------------|----------------|----------------|----------------|----------------|----------------|-----------------|
| 10     |               |               | 0.092          | 0.153          | 0.199          | 0.271          | 0.377          | 0.561           |
| 16     | 0.104         | 0.628         | 0.977          | 1.231          | 1.439          | 1.784          | 2.325          | 3.310           |
| 25     | 0.348         | 0.937         | 1.400          | 1.743          | 2.029          | 2.503          | 3.249          | 4.612           |
| 40     | 0.500         | 1.059         | 1.556          | 1.934          | 2.250          | 2.773          | 3.597          | 5.104           |
| 64     | 0.617         | 1.097         | 1.577          | 1.956          | 2.273          | 2.803          | 3.636          | 5.158           |
| 100    | 0.699         | 1.093         | 1.523          | 1.877          | 2.180          | 2.688          | 3.489          | 4.952           |
| 160    | 0.766         | 1.075         | 1.435          | 1.746          | 2.018          | 2.484          | 3.227          | 4.584           |
| 250    | 0.814         | 1.056         | 1.349          | 1.611          | 1.846          | 2.258          | 2.928          | 4.164           |
| 400    | 0.854         | 1.039         | 1.270          | 1.480          | 1.674          | 2.020          | 2.601          | 3.697           |
| 640    |               | 1.026         | 1.206          |                | 1.526          | 1.808          | 2.293          |                 |
| 1,000  |               | 1.018         | 1.159          |                | 1.413          | 1.639          | 2.036          |                 |
| 1,600  |               | 1.012         | 1.121          |                | 1.318          | 1.496          | 1.811          |                 |
| 2,500  |               | 1.008         | 1.093          |                | 1.248          | 1.389          | 1.639          |                 |
| 4,000  |               | 1.005         | 1.071          |                | 1.192          | 1.301          | 1.496          |                 |
| 6,400  |               | 1.003         | 1.055          |                | 1.148          | 1.233          | 1.386          |                 |
| 10,000 |               | 1.002         | 1.043          |                | 1.117          | 1.301          | 1.304          |                 |

<sup>a</sup>Values calculated from Equations (6) and (7).

TABLE III

EXPERIMENTAL RESULTS AND CALCULATED HYDRODYNAMIC PARAMETERS  
 FOR GUARAN TRIACETATE IN ACETONITRILE AT 25°C.

| Fraction | $\bar{N}_w$ | $[\eta]$ ,<br>ml./g. | $\bar{h}$ | $\frac{q_0}{\bar{N}_w}$ | $\bar{S}^2 \times 10^{-4}$ ,<br>A <sup>2</sup> , a | $\Phi \times 10^{-23}$ ,<br>mole <sup>-1</sup> |
|----------|-------------|----------------------|-----------|-------------------------|--|--|
| 2A       | 12,400      | 945                  | 4.00      | 1.35                    | 147  | 2.61   |
| 2B       | 11,200      | 912                  | 4.00      | 1.35                    | 133  | 2.66   |
| 3        | 7,640       | 703                  | 3.03      | 1.44                    | 94.2   | 2.49   |
| 4        | 6,200       | 678                  | 5.10      | 1.28                    | 71.3   | 2.62   |
| 2C       | 4,770       | 560                  | 4.00      | 1.35                    | 56.4   | 2.50   |
| 5        | 1,970       | 387                  | 12.4      | 1.13                    | 20.7   | 2.69   |
| 6        | 764         | 179                  | 33.3      | 1.04                    | 7.47   | 2.05   |
| 7        | 532         | 116                  | 45.7      | 1.03                    | 5.07   | 1.64   |
| 8        | 171         | 44                   | 11.1      | 1.14                    | 1.54   | 1.32   |

<sup>a</sup>Calculated from Equation (12) using a persistence length of  $\bar{a} = 57.8 \text{ \AA}$ .

calculated from light scattering molecular weights obtained in a Brice-Phoenix light scattering photometer. The values are based on an average monomer molecular weight of 432.

The polymolecularity of the GTA fractions has been estimated from osmotic pressure and ultracentrifuge measurements. The results are expressed in terms of the Zimm-Schulz (10) parameter  $h$  and the number and  $z$ -average degrees of polymerization may be calculated from the relation,

$$\frac{h}{\bar{N}_n} = \frac{h+1}{\bar{N}_w} = \frac{h+2}{\bar{N}_z}, \quad (8)$$

where  $\bar{N}_n$ ,  $\bar{N}_w$ , and  $\bar{N}_z$  are respectively the number, weight and  $z$ -average degrees of polymerization.

#### MOLECULAR PARAMETERS FROM INTRINSIC VISCOSITY

In treating intrinsic viscosity data, Eizner and Ptitsyn rearrange Equation (2) to yield,

$$2^{3/2} \frac{b^3}{M_0} \frac{N}{[\eta]} \chi_{(N/\lambda)} = \left(\frac{2\pi}{3}\right)^{1/2} \frac{45}{32(3-2^{1/2})} \frac{b}{\lambda r_0} + \frac{1}{\lambda^{3/2}} \varphi(\lambda/N) N^{1/2} \quad (9)$$

which is of the form,  $Y = A + BX$ . A plot of  $Y = 2^{3/2} \frac{b^3}{M_0} \frac{N}{[\eta]} \chi_{(N/\lambda)}$  versus  $X = \frac{1}{\lambda^{3/2}} \varphi(\lambda/N) N^{1/2}$  should be a straight line providing an appropriate value of  $\lambda$  is used. Initial values of  $\lambda_1$  were assumed and from a least squares treatment of the data according to Equation (9) a final value of  $\lambda_f$  was calculated. The procedure was repeated several times and a correct value of  $\lambda$  was determined from the intersection of the curve relation  $\lambda_1$  to

$\lambda_{\underline{f}}$  with the straight line,  $\lambda_{\underline{i}} = \lambda_{\underline{f}}$ . Values of  $\chi(\underline{z})$  and  $\Psi(\lambda, \underline{N})$  were obtained from graphs of  $\Psi(\lambda, \underline{N})$  versus  $\underline{N}$  and  $\chi(\underline{z})$  versus  $\underline{z}$  which were prepared on the basis of the data given in Tables I and II.

The final results are shown in Figure 1 for the correct value of  $\lambda = 11.2$  based on a value of 5.15 A. for the length of the monomer unit  $\underline{b}$ . The straight line as determined by the method of least squares is given by,  $\underline{y} = 0.194 + 0.0266\underline{x}$ . The persistence length obtained from  $\lambda$  is  $\underline{a} = 57.8$  A. which is only slightly lower than the limiting value of 64 A. obtained from light scattering (1). A value of  $\underline{r}_0 = 3.04$  A. is obtained for the radius of the monomer unit, and the ratio  $\underline{C}/\eta_0 = 6\pi\underline{r}_0$  is 57.3 A.

Since all important parameters are known, Equation (2) may be used to calculate the dependence of intrinsic viscosity on degree of polymerization as shown in Figure 2. The circles represent experimental data and the solid line represents the intrinsic viscosity calculated from Equation (2). It is apparent that the agreement between theory and experiment is excellent.

#### THE FLORY COEFFICIENT

The Eizner-Ptitsyn theory can also be used to predict the dependence of the Flory coefficient on degree of polymerization according to Equation (4). The Flory coefficient may also be calculated from experimental data using the relation, (1),

$$\bar{\Phi} = q_0 [\eta] \bar{M}_w / (6 \bar{S}_z^2)^{3/2} \quad (10)$$

where  $\bar{M}_w$  is the weight average molecular weight,  $\bar{S}_z^2$  is the z-average mean-square radius-of-gyration and  $q_0$  is a factor to correct for sample

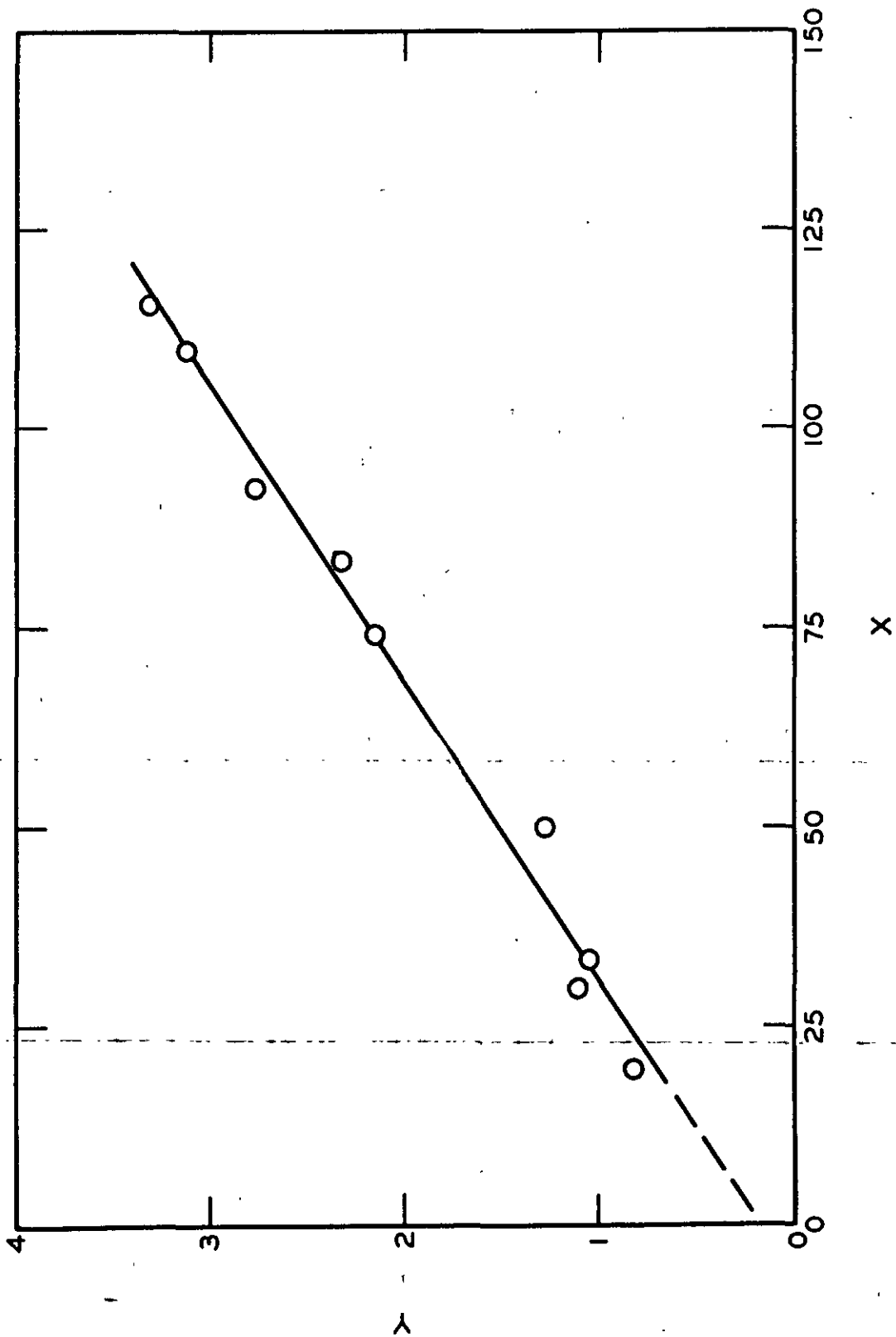


Figure 1. Intrinsic viscosity data for guaran triacetate in acetonitrile treated according to the Eizner-Ptitsyn theory for the semirigid macromolecule. Open circles and straight line based on  $\lambda = 11.2$ .

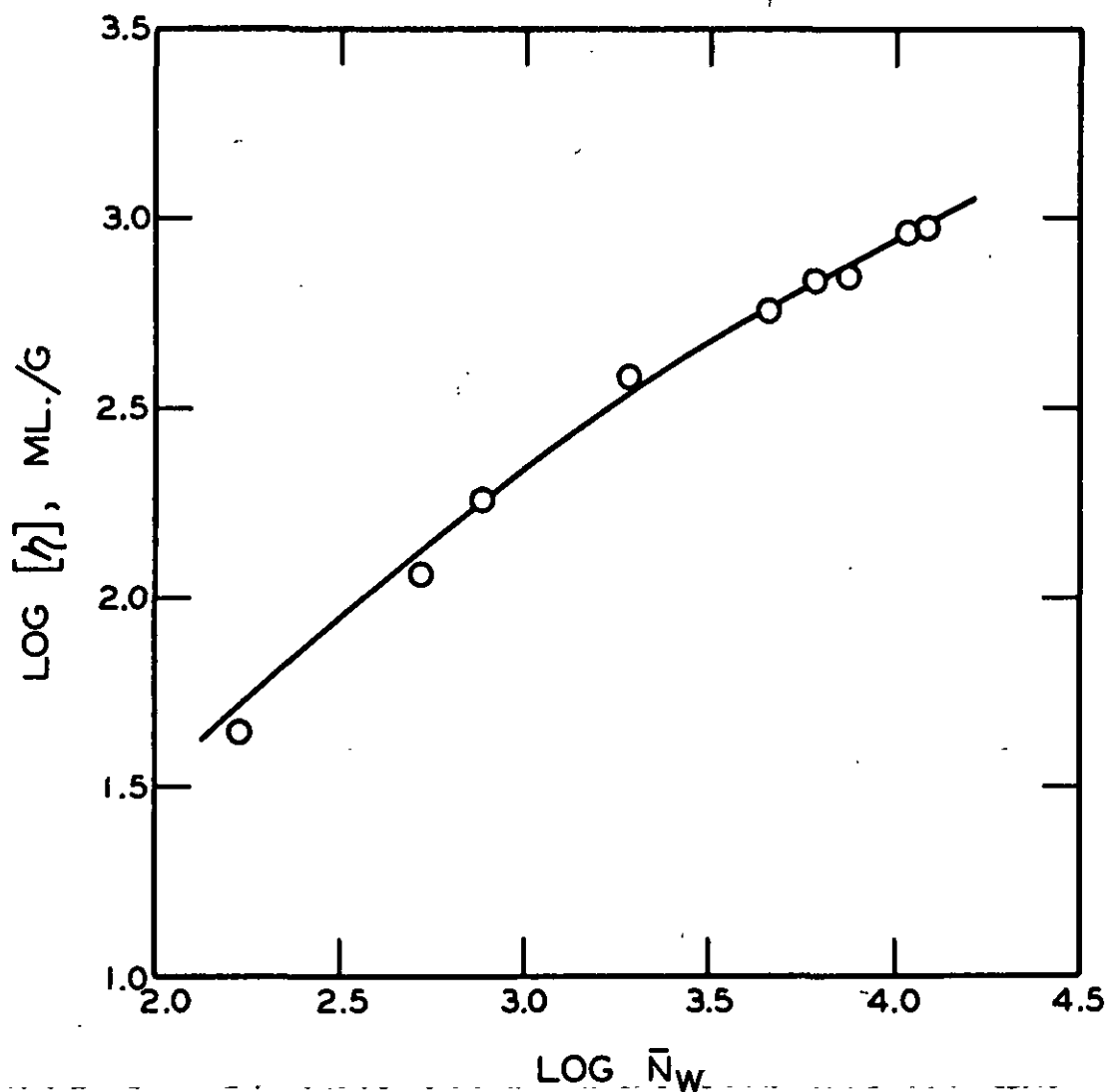


Figure 2. Intrinsic viscosity as a function of weight average degree of polymerization for guaran triacetate in acetonitrile. Open circles represent experimental data. The solid line is the theoretical Eizner-Ptitsyn curve, calculated from Equation (2).

heterogeneity. For a distribution of the Zimm-Schulz type,  $q_0$  is given by (1),

$$q_0 = (h + 2)^{3/2} \Gamma(h+2) / (h + 1)^2 \Gamma(h+1.5). \quad (11)$$

Since the persistence length of the GTA molecule is known from hydrodynamic measurements, the radius of gyration may be calculated from (1),

$$\overline{(S_z^2)} = a^2 [(\overline{N}_z b / 3a) - 1 + (2a/\overline{N}_w b)(1 - (a/\overline{N}_n b))]. \quad (12)$$

Values of the Flory coefficient calculated from experimental data are given in Table III. It should be noted from the magnitude of  $q_0$  that appreciable heterogeneity corrections are required.

The dependence of the Flory coefficient on degree of polymerization is shown in Figure 3. The circles represent values calculated on the basis of Equations (10) (11) and (12) and experimental data while the solid line represents the theoretical curve calculated from Equation (4). Here again the agreement between theory and experiment is good.

#### DISCUSSION

A number of hydrodynamic theories are available and have been tested in the course of the present investigation. The excluded volume theory of Kurata and Yamakawa (7) has been used by Koleske (1) in his analysis of the hydrodynamic behavior of GTA. In his work, excluded volume effects were shown to be unimportant so that the theoretical equations of the Kurata-Yamakawa theory reduce to those of Kirkwood and Riseman (6). More recently, Hearst (8) has modified the theory of Zimm (11)

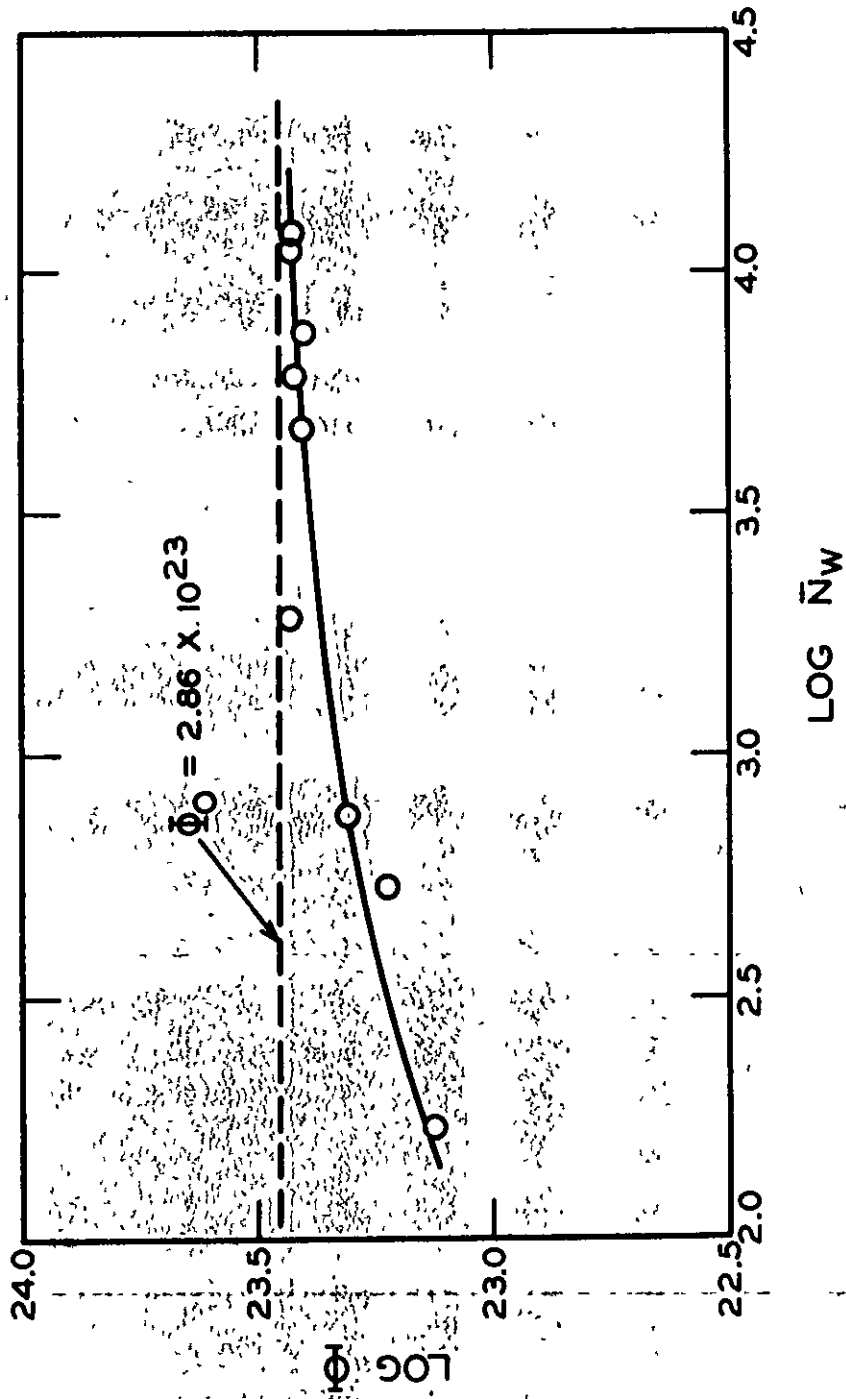


Figure 3. The Flory coefficient as a function of weight average degree of polymerization for guaran triacetate in acetone-triethylamine. Circles represent experimental data. The solid line is the theoretical Eizner-Ptitsyn curve calculated from Equation (4).

to determine the effect of partial draining on the intrinsic viscosity of flexible macromolecules.

All of these theories were considered in the present investigation and while they predict the observed hydrodynamic behavior at high molecular weight, they fail in a quantitative sense at lower molecular weights. At low molecular weights a constant value of the monomeric friction coefficient will not describe the observed dependence of intrinsic viscosity on molecular weight. The Eizner-Ptitsyn theory appears to be free of this difficulty and indeed leads to a reasonable value for the hydrodynamic radius of a monomer unit and the persistence length.

LITERATURE CITED

1. Koleske, J. V. The configuration and hydrodynamic properties of fully acetylated guaran. Doctor's Dissertation. Appleton, Wisconsin. The Institute of Paper Chemistry, 1962. 175 p.
2. Eizner, Yu. E., and Ptitsyn, O. B., Vysokomol. Soed. 4:1725 (1962).
3. Peterlin, A., J. Polymer Sci. 5:473 (1950).
4. Peterlin, A., J. Chem. Phys. 33:1799 (1960).
5. Kratky, O., and Porod, G., Rec. Trav. Chim. 68:1106 (1949).
6. Kirkwood, J. G., and Riseman, J., J. Chem. Phys. 16:265 (1948).
7. Kurata, M., and Yamakawa, H., J. Chem. Phys. 29:311 (1958).
8. Hearst, J. E., J. Chem. Phys. 37:2547 (1962).
9. Flory, P. J., and Fox, T. G., Jr., J. Am. Chem. Soc. 73:1904 (1951).
10. Schulz, G. V., Z. phys. Chem. 843:25 (1939).
11. Zimm, B. H., J. Chem. Phys. 24:269 (1956).